Raman scattering intensity of the long-period polytypes of CdI_2

S. Nakashima, H. Katahama, Y. Nakakura, and A. Mitsuishi
Department of Applied Physics, Osaka University, Yamada-oka, Suita, Osaka 565, Japan

B. Pałosz
Institute of Physics, Warsaw Technical University, PL-00-662 Warszawa, ul. Koszykowa 75, Poland
(Received 26 November 1984)

Raman scattering measurements have been made on the long-period polytypes of CdI_2 whose structure has been identified by x-ray diffraction analysis. In addition to the principal phonon modes, we have observed new shear-type Raman modes which result from zone-folding effects. It is found that the relative Raman intensities of these folded modes depend strongly on the structure of the polytypes. A simple model is presented to explain the Raman intensity profiles of these polytypes. Model calculations of the relative Raman intensity show a qualitative agreement with the observations. The absence of folded modes of the compressional type is also explained by the model. It is shown that the Raman intensity profiles can be used to identify the structure of CdI_2 polytypes. Finally, the model and the results of the analysis are discussed.

I. INTRODUCTION

Layered crystals are constructed by stacking identical layers which are connected by weak interlayer interactions. Some layered crystals crystallize in different modifications which differ only in the stacking arrangement of the identical unit layers. This phenomenon is called polytypism.[1] Polytypism is widely observed in layered crystals with weak interlayer interactions such as CdI_2, PbI_2, $CdBr_2$, SnS_2, GaSe, and also in the covalent crystals of SiC. The polytype is a form of a "natural superlattice."

The Raman spectra of different polytypes have been measured in CdI_2,[2,3] PbI_2,[4–8] SnS_2,[9–11] GaSe,[12–15] and SiC.[16,17] Recently, we have measured the Raman spectra of various polytypes of CdI_2.[3,18] These polytypes have shown several new Raman bands which arise from the folding of the Brillouin zone of the single-layer polytype ($2H$ polytype). The new modes resulting from the folding of dispersion curves to the Γ point are referred to as folded modes and the unfolded Brillouin zone will be called the basic zone.[19] The dispersion curves of the transverse-acoustic (TA) phonons propagating along the c direction have been determined from the frequencies of the folded TA modes which are known as shear-type rigid-layer (RL) modes.

In the course of the Raman study of CdI_2 polytypes, peculiar features have been found in the spectra of several polytypes: The relative intensities of the shear-type RL modes and the intralayer modes depend strongly on the structure of the polytype.[3] Also some folded and/or unfolded modes are missing. A typical example is the $4H$ polytype. Group theory predicts the presence of E_1 and E_2 Davydov partners of the intralayer mode in the $4H$ polytype, but only the E_2-type mode has been observed.[20] For all the polytypes measured so far, the compression-type (A-type) RL modes are too weak to be observed. This observation suggests that there exist some rules for the Raman intensity of CdI_2 polytypes in addition to the usual selection rules obtained from the group-theoretical analysis.

So far little attention has been paid to the Raman intensity of layered crystals. Raman spectra of the Davydov pairs for optic modes have been observed in PbI_2, GaSe, and SnS_2. However, no systematic study has yet been made on this subject. Schmid[21] has explained the relative intensity of the E-type Davydov doublet in $4H$-PbI_2 where the E_1 band is weaker than the E_2 band[22] but both E_1 and E_2 bands are observed in contrast to the case of $4H$-CdI_2. He has pointed out that the Raman tensor components α_{xz} and α_{yz} for the E_1 mode arising from layers 1 and 2 cancel out if the total Raman components for the primitive unit cell are the sum of the components for each layer in the cell, whereas the α_{xx}, α_{yy}, and α_{xy} components do not cancel. This cancellation or nonvanishing behavior is a consequence of the symmetry of the $4H$ polytype.

A similar argument has been applied by Polian *et al.* to the E'' Davydov doublet observed at about 59 cm^{-1} in ϵ-type GaSe, in which the primitive unit cell contains two layers and there is no symmetry operation transferring one layer into another.[14] They have proposed that the net Raman tensor is vanishingly small for the antisymmetric mode of the Davydov pair because cancellation occurs between the contributions from two layers and hence the Raman intensity is very weak. Their conclusion is not a consequence of the crystal symmetry but the molecular nature of the GaSe-layered crystal, where the Raman tensor components and the displacement amplitudes are assumed to be the same for each layer.

In this work we have observed the Raman spectra of various polytypes of CdI_2. A simple model has been proposed in order to explain the relative intensity of the Raman bands in these polytypes. In this layered-crystal model, the vibrational amplitudes of individual layers for folded modes are not necessarily equal and have certain values equal to that of corresponding phonon modes

within the basic zone. On the basis of this model the relative intensity profile of the folded modes of the transverse-acoustic and optic branches in the Δ direction are qualitatively explained.

In Sec. II, we describe the preparation of the polytype crystals and the experimental procedures. In Sec. III, we present the results of the Raman measurements. The dispersion curves of the shear-type acoustic and optic phonons in the basic zone are estimated in Sec. III C. In Sec. IV, we present a model based on the bond polarizability concept and calculate the relative Raman intensity of the polytypes. In Sec. V, we compare the computed Raman intensities with the observed Raman intensity profiles. In Sec. VI, we discuss the application of our model to other layered crystals.

II. EXPERIMENTAL

The CdI_2 polytypes used in this experiment were grown from an aqueous solution and mixed solution of ethanol and water. The $4H$ polytype is a structural modification of CdI_2 which is most frequently observed. Melt-grown crystals exhibit predominantly the $4H$ polytype, while higher-ordered polytypes other than $4H$ are occasionally found in the solution growth. Systematic studies were made of the structure of CdI_2 crystals grown from an aqueous solution and from mixed solutions.[23–26] Solution-grown crystals were hexagonal plates typically a few hundred μm thick.

The structures of the polytypes were determined by x-ray diffraction measurements. A cylindrical camera of 43-mm radius, a collimator of aperture 0.5 mm and Cu K Ni-filtered radiation were used. The crystals were oscillated around the a axis in the range 19°—34°. This equipment provides information only about thin surface layers of the polytypes because the x rays penetrate a surface layer of about 30 μm. The structure of the whole volume of polytypes was estimated from the analysis of the two opposite basal planes of the crystals. The detailed method for the determination of the layer stacking is described in Ref. 27.

Polytype conversion was sometimes observed after cooling and heating procedures in the low-temperature measurements. It was not observed for room-temperature measurements. When spectra different from the initial spectra were found, the crystal was reexamined by the x-ray measurement. Many polytypes used in this experiment were found occurring with other structures, frequently in the presence of the basic structure of the $4H$ polytype. Only a few specimens had uniform structure and were pure polytypes. Table I lists the polytypes used in the comparison between experimental and calculated results.

Several notations have been proposed in order to represent the structure of the polytypes. Ramsdell notation, $2nH$ and $6nR$, is commonly used to indicate the period of the stacking layers, although the notation is not convenient to describe the layer structure. Besides this, there are Zhdanov notation,[1] *ABC* sequence,[1] t-o-f notation,[28] and so on. In the present analysis we will use mainly the *ABC* sequence, which shows directly the relative configuration of each layer.

In the CdI_2 structure constituent atoms are close packed and there are three possible positions for a given atomic plane, which are denoted by A,B,C, or α,β,γ. The Latin and Greek letters represent iodine and cadmium planes, respectively. The $4H$ polytype is written as $(A\gamma B)(C\alpha B)$ or $(AB)(CB)$. The Greek letters are often omitted since the position of a Cd plane is uniquely determined if two iodine planes within a layer are given.

Raman spectra were excited with an argon-ion laser operating at 4880 Å with a $\sim$70-μm focused spot size on the sample surface. A backscattering geometry was employed and the spectrum was analyzed using a Spex 1403

TABLE I. Structures of CdI_2 polytypes used in the measurements of Raman intensities. The **q** vectors in the basic zone, which are folded into the Γ point, are also given.

Structure	Zhdanov notation	Space group	Number of layers in primitive unit cell	q of the folded modes $\mathbf{q}=(0,0,q)\pi/c$
$2H$	11	D_{3d}^3 ($P\bar{3}m1$)	1	
$4H$	22	C_{6v}^4 ($P6_3mc$)	2	1
$6H_1$	2211	C_{3v}^1 ($P3m1$)	3	$\frac{2}{3}$
$18R_1$	$[1212]_3$	D_{3d}^5 ($R\bar{3}m$)	3	$\frac{2}{3}$
$8H_3$	1232	D_{3d}^3 ($P\bar{3}m1$)	4	$\frac{1}{2}$, 1[a]
$24R_1$	$[2213]_3$	C_{3v}^5 ($R3m$)	4	$\frac{1}{2}$, 1
$24R_2$	$[212\,111]_3$	C_{3v}^5 ($R3m$)	4	$\frac{1}{2}$, 1[a]
$12H_2$	21 211 212	C_{3v}^1 ($P3m1$)	6	$\frac{1}{3}$, $\frac{2}{3}$, 1
$12H_4$	22 211 211	C_{3v}^1 ($P3m1$)	6	$\frac{1}{3}$, $\frac{2}{3}$, 1
$14H_6$	$22(11)_5$	C_{3v}^1 ($P3m1$)	7	$\frac{2}{7}$, $\frac{4}{7}$, $\frac{6}{7}$
$42R_1$	$[(22)_2 2121]_3$	C_{3v}^5 ($R3m$)	7	$\frac{2}{7}$, $\frac{4}{7}$, $\frac{6}{7}$
$16H_6$	22 212 223	D_{3d}^3 ($P\bar{3}m1$)	8	$\frac{1}{4}$, $\frac{2}{4}$, $\frac{3}{4}$, 1[a]
$20H_{14}$	$(22)_2 12\,212\,211$	C_{3v}^1 ($P3m1$)	10	$\frac{1}{5}$, $\frac{2}{5}$, $\frac{3}{5}$, $\frac{4}{5}$, 1
$22H_4$	$(211)_2 22\,112\,222$	C_{3v}^1 ($P3m1$)	11	$\frac{2}{11}$, $\frac{4}{11}$, $\frac{6}{11}$, $\frac{8}{11}$, $\frac{10}{11}$

[a]Raman inactive.

double monochromator. A microcomputer was used for data acquisition and scanning control of the monochromator. The frequencies of the Raman bands were always determined by recording both anti-Stokes and Stokes components in successive scans passing through the Rayleigh peak and by averaging both Raman shifts. This procedure compensated the zero shift of the spectrometer and gave more reliable frequency values with an accuracy better than ± 0.1 cm^{-1}. For the measurement of low-lying modes with frequencies less than 5 cm^{-1}, an I_2 cell was used to eliminate the stray light. For measurement at liquid-He temperature, samples were immersed in liquid He in a conventional glass cryostat. No polarization measurement was made.

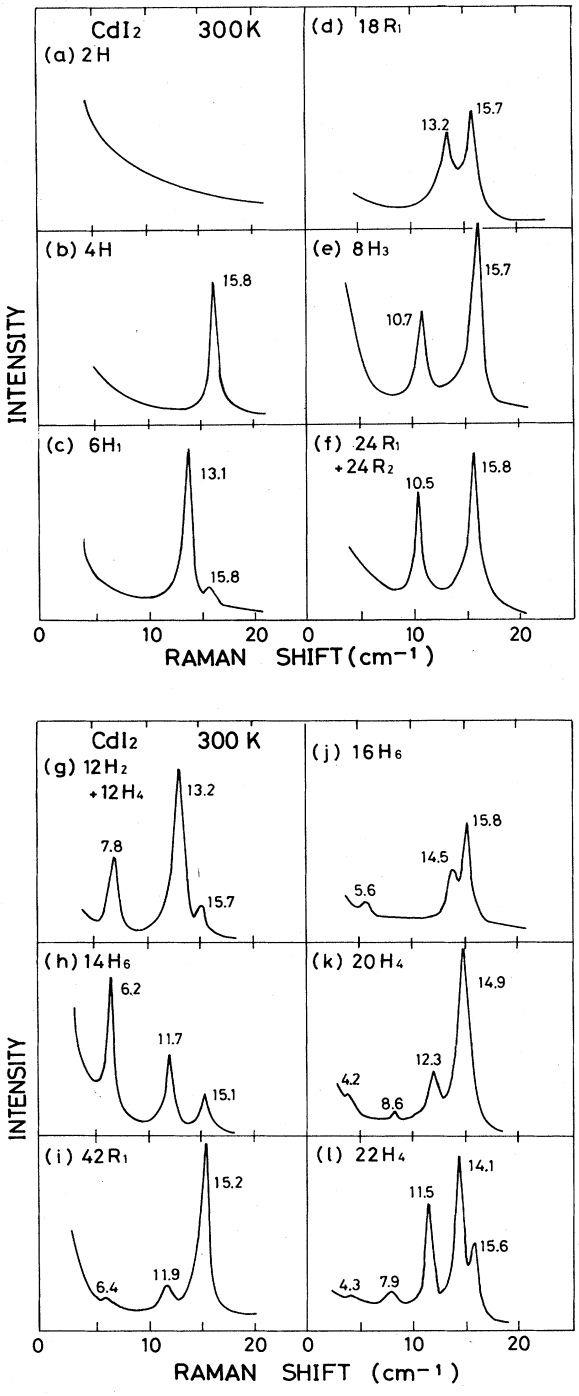

FIG. 1. Low-frequency portion of Raman spectra for various polytypes of CdI_2. The numbers in the figures are the frequencies of the Raman bands.

III. EXPERIMENTAL RESULTS

A. Interlayer modes

Figure 1 shows the room-temperature Raman spectra of shear-type interlayer modes for various polytypes. These Raman bands corresponding to the folded modes of the transverse acoustic branch are symmetric and narrow (less than 2 cm^{-1} in width at 300 K). The relative intensity of the folded bands depends on the structure of the polytype. The intensity profiles are different even for the polytypes with the same periodicity if their stacking structures are different ($14H_6$ and $42R_1$). A band at 15.8 cm^{-1} corresponding to the zone-edge phonon mode in the $2H$ polytype is Raman active for the polytypes, $4H$, $24R_1$, $12H_2$, $12H_4$, and $20H_{14}$. This mode is only infrared active for the polytypes $8H_3$, $24R_2$, and $16H_6$, because these polytypes have inversion centers within a layer. As shown in Fig. 1, the forbidden band at 15.8 cm^{-1} is observed for the polytypes $6H_1$, $8H_3$, and $42R_1$. We believe this is due to the coexistence of the $4H$ polytype in these polytype samples. The relative intensity of Raman bands in the $8H_3$ polytype varies with the position irradiated by the exciting laser beam. This effect arises from the structural inhomogeneity of the crystal samples. Such position dependence was also observed in other composites of polytypes. In addition to the samples listed in Table I, a number of higher polytypes have been examined. Since the majority of those specimens contain predominantly the $4H$ polytype, the intensities of the folded modes are too weak to be compared. Only the peak frequencies have been examined.

The folded modes corresponding to a mode within a basic zone consist of a doublet. Both partners of the doublet are Raman active if the polytype belongs to one of the noncentrosymmetric space groups C_{3v}^1, C_{3v}^5, or C_{6v}^4. Careful measurements were made at 4.2 K in order to determine the splitting of the doublets. Neither splitting nor deviation from a single Lorentzian shape was observed. This result suggests that the folded modes corresponding to a given mode within the basic zone are essentially degenerate in CdI_2. The folded modes of the longitudinal acoustic branch are expected to appear from the group-theoretical analysis. However, these modes were not observed despite careful measurements.

B. Intralayer modes

The folded intralayer bands have been measured at liquid-He temperature, because the intralayer Raman bands are so broad at room temperature that each component cannot be resolved. Figure 2 shows the Raman spectra of the E-type intralayer modes in the frequency range 50—60 cm^{-1} for several polytypes. The spectral

features of these modes depend strongly on the polytype structure as for the interlayer modes. For the $2H$ polytype, a weak band is observed at about 51.4 cm^{-1}. It may be due to the $4H$ polytype contained partly in this crystal. It is to be noted that only a band at 51.4 cm^{-1} is observed for the $16H_6$ polytype, although four Raman-active modes are expected from group-theoretical analysis. Some modes of the A_{1g} optic branch, which are expected to appear, were not observed presumably because of their extremely weak intensity. The folded modes of the A_{2u} and E_u optical branches were also missing.

We tried to observe the E_1-type Raman band at 57.4 cm^{-1} in the $4H$ polytype for the right-angle scattering configuration, because this mode is forbidden in the back-scattering configuration employed here. However, the E_1 band is too weak to be observed. We have concluded from this observation that the intensity of the E_1 band is less than one-thousandth of the Raman intensity of the E_2 band.

C. Phonon dispersion curves

The dispersion curves in the Δ direction in the basic zone can be estimated from the frequencies of the observed folded modes. Since in CdI_2 the frequency of the E-symmetry intralayer mode is relatively low, admixture between the intralayer and interlayer modes should be considered in order to interpret the dispersion relations.[3] In this paper we will make our analysis considering the admixture of both forces in the framework of the linear-chain model. This model contains (i) the interlayer forces between the nearest-neighbor iodine atoms f_1 and between the second-nearest-neighbor iodine atoms f_2, and (ii) the intralayer forces between cadmium and iodine F_1 and between iodine atoms in opposite atomic planes in a layer F_2. In Fig. 3 the calculated curves are shown by solid lines. The calculation reproduces well the experimentally determined dispersion curves. The fitting parameters chosen here are $f_1=2.1\times10^3$, $f_2=-0.2\times10^3$, $F_1=1.5\times10^4$, and $F_2=2.75\times10^3$ dyn/cm at 4.2 K, and $f_1=1.68\times10^3$, $f_2=-0.15\times10^3$, $F_1=1.5\times10^4$, and $F_2=5\times10^2$ dyn/cm at 300 K. Deviation of the experimental value from the fitting curve is less than ±0.3 cm^{-1} for all RL Raman bands. The ratio between interlayer and intralayer force constants f, F (~10) is small compared with those of other layered crystals ($\sim10^2$–10^3). This small ratio arises from relatively weak intralayer forces in CdI_2, since the interlayer force of an order of 10^3 dyn/cm is comparable to that of other layered crystals.

In our linear-chain model only short-range forces are considered. However, it has been pointed out that the interlayer modes in the CdI_2-type crystals are affected by the long-range interaction due to the static dipoles of anions.[29,30] We have recently made an analysis of the Raman frequencies based on the polarizable-ion model[29] in $2H$- and $4H$-CdI_2. The calculated frequencies were in agreement with the experimental values for both polytypes. The analysis showed that the absolute frequency

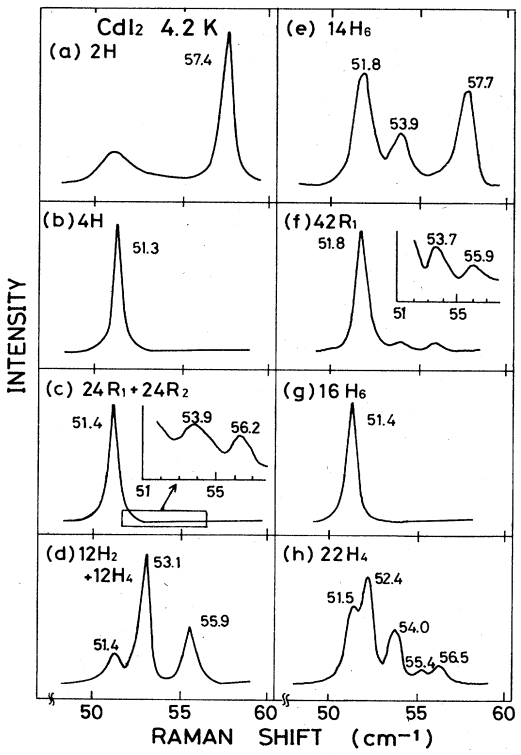

FIG. 2. Raman spectra of CdI_2 polytypes in the high-frequency portion, which were observed at 4.2 K.

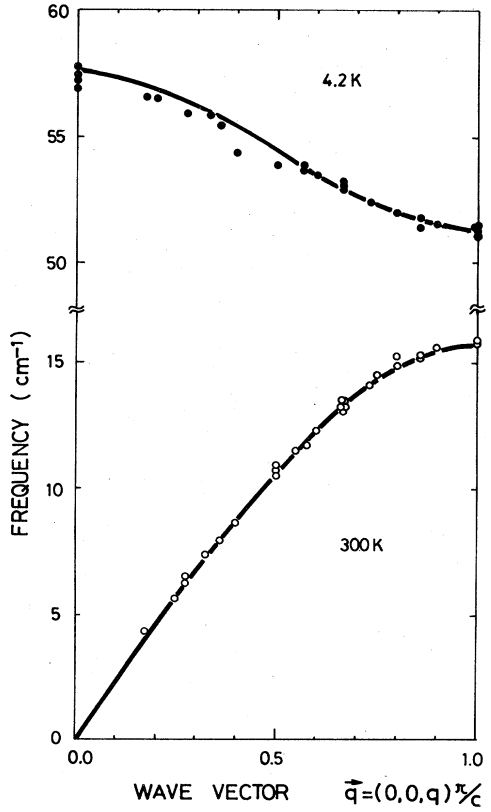

FIG. 3. Estimated dispersion curves of the shear-type acoustic and optic phonons in the [00ξ] direction. The frequencies of optical and acoustic branches are obtained at 4.2 and 300 K, respectively. Solid lines are calculated from linear chain model using force-constant values taken in the text.

values were sensitive to the long-range forces but that the frequency difference between the E modes of the $2H$ and $4H$ polytypes and hence the frequency difference between the zone-center and zone-edge phonons in the basic zone were little affected by the long-range forces. This result seems to ensure the use of the linear-chain model with short-range force constants in the description of the dispersion curves if the effect of the long-range force is included in the force constants. The detailed analysis of the dispersion curves will be reported elsewhere.[18]

IV. DESCRIPTION OF THE MODEL: INTERATOMIC POLARIZABILITY TREATMENT

A. Shear-type modes

Interatomic forces in layered crystals are classified into interlayer and intralayer forces, whose magnitudes are widely different from each other. The ratio of the interlayer to intralayer forces estimated from experiments lies between 10^{-2} and 10^{-3} for typical layered crystals. The vibrational modes of the layered crystals are characterized by the contribution of the two forces. The restoring forces of acoustic phonons propagating along the c direction are dominated by the weak interlayer forces. For these phonon modes all the atoms within a layer move with the same phase and amplitude and then these phonon modes form the so-called rigid-layer (RL) modes. On the other hand, the contribution of the intralayer forces is dominant for optic modes.

From the nature of the vibrational modes in the layered crystals, the atomic displacements of folded modes in higher-order polytypes are approximated as follows:

(a) First, each layer moves as a rigid unit for all interlayer modes arising from the folding of acoustic branches.

(b) Second, all Raman-active intralayer modes resulting from the folding of optic branches have displacement patterns where two iodine planes in an I-Cd-I layer move symmetrically and a cadmium plane is at rest as shown in Fig. 4. In other words, for the folded modes in the higher polytypes, the displacement pattern within a layer is the same as that of the $2H$ polytype (isolated-layer approximation).

(c) Third, for both folded interlayer and intralayer modes, vibrational amplitudes of respective layers are equal to those of the corresponding modes in the $2H$ polytype which have a definite wave vector (wavelength).

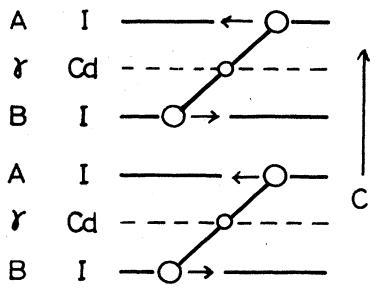

FIG. 4. Displacement pattern for the shear-type intralayer mode in $2H$ polytype.

The relative Raman intensity of the folded modes depends on the atomic displacement relevant to these modes (normal coordinates) and the polytype structure. Raman scattering intensity is proportional to the square of the differential polarizability, i.e., the polarizability derivative with respect to normal coordinates.

The differential polarizability $\alpha'=(\partial\alpha/\partial Q)_0$ of the folded intralayer modes can be derived under the following assumptions:

(i) The contribution to the differential polarizability from the relative displacement between iodine atoms in the adjacent layers is very small.

(ii) The contribution to the differential polarizability arises mainly from the relative displacements of the iodine plane from the cadmium plane.

(iii) The differential polarizability of isolated layers is the same for any layer structures. The cancellation of the differential polarizability occurs for any pair of I-Cd-I layers if the relative displacements for the two layers are out of phase with each other.

The assumption (i) is not unreasonable considering the fact that the Raman intensity of the RL modes is about one-fifth of that of the E_2 type intralayer mode in the pure $4H$ polytype after Bose-factor correction.

In (ii) we have considered only the relative displacements of I-Cd planes. There would be another contribution from the displacement of I-I planes within a layer. However, it may be small compared with that of the I-Cd displacement.

If we consider a pair of the layer ($A\gamma B$), whose displacements along the [210] direction are shown in Figs. 5(a) and 5(b), the combination of the relative displace-

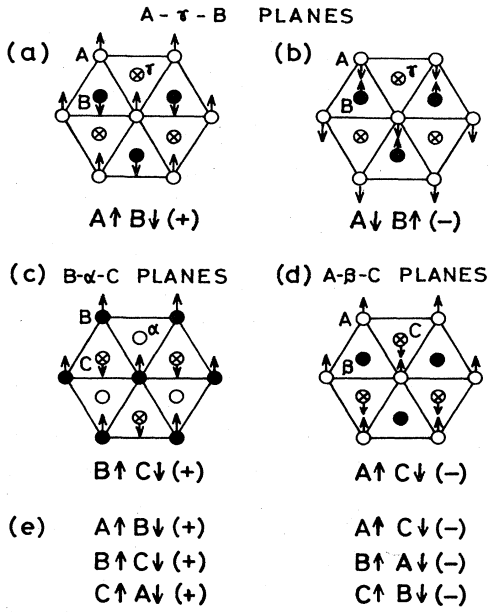

FIG. 5. Relative displacements of three pairs of iodine planes along the ⟨210⟩ direction. (a) Displacement of A-B planes, (b) counterphase displacement of (a), (c) displacement of B-C planes, (d) displacement of A-C planes, and (e) the determination of the sign for the relative displacements of iodine planes. This definition is applicable to iodine planes within a layer and also to the interlayer I-I′ planes. See text.

ments $(A\uparrow B\downarrow)(A\downarrow B\uparrow)$ does not differ in its pattern for the counterphase displacement $(A\downarrow B\uparrow)(A\uparrow B\downarrow)$. Hence, the polarizability $\alpha(Q_i)$ is an even function of displacement Q_i and the differential Raman polarizability $\alpha'=(\partial\alpha/\partial Q_i)_0$ is zero. This argument applies to the displacements along any direction within the basal plane. This cancellation of the Raman polarizability can occur for any combinations of layers (AB), (AC), and (BC). It is to be noted that the contributions to the Raman polarizability from two double planes within a layer [e.g., A-γ and γ-B within the layer $(A\gamma B)$] are always additive.

The Raman polarizability for the relative displacement of neighboring atomic planes is proportional to the displacement amplitude. It can be explained as follows: The zone-center phonon modes in the $2H$ polytype are represented by nine normal coordinates or nine symmetry coordinates. For $2nH$ and $6nR$ polytypes, $9n$ normal coordinates are constructed from the linear combination of symmetry coordinates which correspond to the atomic displacements within a layer in the $2H$ polytype. The differential polarizability can be expressed in terms of the polarizability derivatives with respect to the symmetry coordinates:

$$\frac{\partial\alpha}{\partial Q_l}=\sum_i\frac{\partial\alpha}{\partial S_i}\frac{\partial S_i}{\partial Q_l}=\sum_i u_{il}\frac{\partial\alpha}{\partial S_i}\ , \tag{1}$$

where the normal coordinates Q and the symmetry coordinates S are related by the transformation

$$S=UQ=[u_{ij}]Q\ . \tag{2}$$

From orthonormality condition, we obtain

$$Q=U^{-1}S=U^{T}S\ . \tag{3}$$

Equation (1) shows that the differential polarizability arising from the displacements for each layer contributes to the Raman polarizability of the lth mode at a rate of u_{il}, which represents the displacement amplitude for the ith layer. Since cadmium atoms are at rest for Raman-active modes, the symmetry coordinates S_i are expressed by the sum of the relative displacements between cadmium and iodine within the ith layer $(x_{\mathrm{I}}^{(i)}-x_{\mathrm{Cd}}^{(i)})+(x_{\mathrm{Cd}}^{(i)}-x_{I'}^{(i)})$. The magnitude of the differential polarizability $\partial\alpha/\partial S_i$ is the same for any layer. Hence, Eq. (1) can be written as

$$\frac{\partial\alpha}{\partial Q_l}=\left|\frac{\partial\alpha}{\partial S_i}\right|\sum_i(\pm)u_{il}\ , \tag{4}$$

where $(\pm)$ signs depend on the layer structure as shown in Fig. 5(e).

The Raman polarizability of the interlayer modes is derived in a similar way. Because the whole layer moves as a rigid unit for the interlayer modes, only the relative displacement of adjacent iodine atoms in the nearest-neighbor layers contributes to the Raman polarizability. The Raman polarizability arising from the relative displacement between the ith and $(i+1)$th layers is given by $\partial\alpha/\partial I_i$, where $I_i=S_i-S_{i+1}$. The net Raman polarizability is expressed by

$$\begin{aligned}\frac{\partial\alpha}{\partial Q_l}&=\sum_{i,j}\frac{\partial\alpha}{\partial I_i}\frac{\partial I_i}{\partial S_j}\frac{\partial S_j}{\partial Q_l}\\&=\sum_i\frac{\partial\alpha}{\partial I_i}(u_{il}-u_{i+1,l})\\&=\left|\frac{\partial\alpha}{\partial I_i}\right|\sum_i(\pm)(u_{il}-u_{i+1,l})\ ,\end{aligned} \tag{5}$$

where $(u_{il}-u_{i+1,l})$ represents the amplitude of the relative displacement between the ith and $(i+1)$th layers.

The net Raman polarizability in a unit cell is determined by the contribution from the Raman polarizability of each pair of neighboring iodine planes, for which the amplitude and the phase of the relative displacement of a pair should be taken into account.

Let us consider first the $4H$ polytype $(AB)(CB)$. The displacement of iodine planes is shown in Fig. 6, where the amplitude varies as $\sin(qc+\delta)$ and δ is a phase angle. The shear-type RL mode corresponds to the zone-edge mode at $(\pi/c)(0,0,1)$ [we will call this mode the "$q(1)$ mode"] of the basic zone. Relative displacements of both neighboring iodine pairs (A-B and B-C) as shown in Fig. 5 contribute additively to the net Raman polarizability. The same is true for the intralayer E_2 mode provided that the influence of C-B and A-B pairs belonging to different layers can be neglected. On the other hand, the contributions from relative displacements of A-γ-B and C-α-B planes cancel out for the E_1 mode, because these displacement patterns have the same amplitude but opposite signs as shown in Figs. 5(a) and 5(e). Therefore, we expect the Raman intensity of the E_1 to be very weak.

The second example is the $16H_6$ polytype, whose ABC sequence is expressed by

$$(AB)(CB)(AB)(C^{*}B)(CA)(CB)(CA)(C^{*}B)\ .$$

This polytype belongs to the space group D_{3d}^{3} and has inversion centers that lie in the Cd planes indicated by an asterisk. The degenerate folded pairs are composed of odd (ungerade) and even (gerade) modes. For Raman-active RL modes, the layer in which the inversion center lies remains at rest as shown in Fig. 7: The displacement patterns are given for E_u and E_g modes corresponding to the $q(\frac{1}{2})$ and $q(\frac{1}{4})$ modes, respectively.

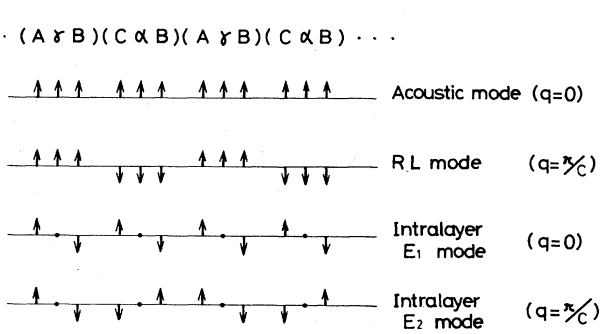

FIG. 6. Normal modes of shear-type vibrations for $q(0)$ and $q(1)$ modes in the $4H$ polytype. The arrow represents the amplitude of vibrations.

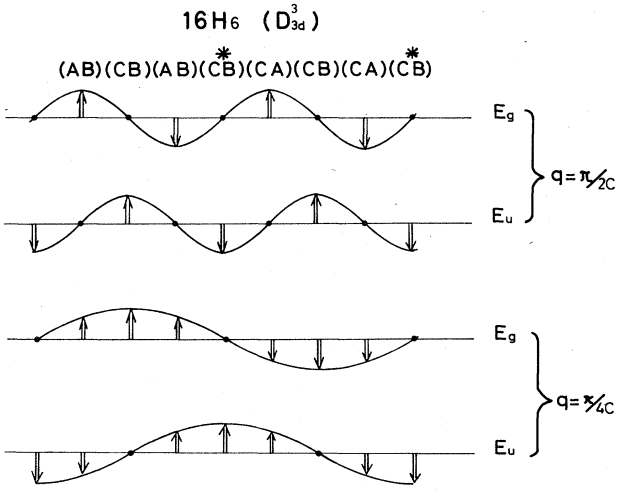

FIG. 7. Normal modes of shear-type vibrations for $q(\frac{1}{2})$ and $q(\frac{1}{4})$ modes in the $16H_6$ polytype.

The Raman polarizabilities arising from the relative displacements of respective pairs cancel out completely for the Raman-active interlayer $q(\frac{1}{2})$ mode and cancel partially for the $q(\frac{1}{4})$ mode. The $q(1)$ mode is an odd mode (E_u symmetry). It can be shown that the net Raman polarizability is always 0 for odd modes. The calculation of the net Raman polarizability of the $16H_6$ polytype yields the result that the Raman polarizability is zero for all intralayer modes except the $q(1)$ mode.

All the folded modes except a mode corresponding to the zone-boundary phonon in the basic zone [$q(1)$ mode] form doublets. They are almost degenerate in CdI_2, because the interatomic forces are essentially independent of the polytype structure. We call this mode a degenerate folded pair. Since the degenerate folded pairs do not interfere with each other, the contribution to the Raman polarizability from a partner of this pair can be calculated independently.

In some polytypes there is no symmetry operation which transfers one layer into another. Such a case is found also in the ϵ-type GaSe.[14] For these polytypes the positions of zero amplitude or phase angle δ are not determined uniquely without solving a dynamical matrix. This means that the net Raman polarizability can not be evaluated uniquely for each partner of the degenerate folded pairs, because the Raman polarizability depends upon the displacement pattern of the iodine planes and its phase angle. This difficulty can be resolved if we consider the sum of the Raman polarizabilities of the pair: For a given degenerate pair the displacement pattern is expressed by a combination of an arbitrary mode $u(\delta)$ and its 90° out-of-phase mode, $u(\delta+\pi/2)$, so that the Raman intensity of a degenerate folded pair is given by the sum of the squared Raman polarizabilities for $u(\delta)$ and $u(\delta+\pi/2)$. It is easily shown that the sum is always independent of the phase angle. Therefore, the choice of the phase angle does not affect the total Raman intensity of the folded pair.

The net Raman polarizabilities of the lth mode in the polytype which contains n layers in the unit cell are given by the following equations; for the intralayer modes,

$$\alpha_l' = \frac{1}{n}\sum_s (\pm)\alpha_s'^{(l)} = \frac{Al}{n}\sum_s (\pm)u_{sl} \ , \tag{6}$$

and for the interlayer modes,

$$\alpha_l' = \frac{Bl}{n}\sum_s (\pm)(u_{sl} - u_{s+1,l}) \ , \tag{7}$$

where s runs over all layers in the unit cell. The real or imaginary part of $u_{sl} = (u_0^{(l)})\exp[i(qx_s+\delta)]$ represents the displacement amplitude for the sth layer, and A_l and B_l are the constants associated with the Raman polarizability arising from the relative displacement for a set of nearest-neighbor planes. Equations (6) and (7) provide Raman polarizabilities per unit volume. The choice of sign in Eqs. (6) and (7) is shown in Fig. 5(e). The Raman scattering intensity σ per unit volume which is proportional to the square of the Raman polarizability is given by

$$\sigma_l \propto |\alpha_l'|^2 \ . \tag{8}$$

This equation includes contributions from the degenerate folded pair. Furthermore, Eqs. (6)—(8) are also applicable to the $q(1)$ mode which is not degenerate, because all displacements of the atomic planes are zero for the motion whose phase angle deviates from that of the $q(1)$ mode by 90°, and its contribution is 0.

We have calculated the relative Raman intensity of the intralayer and interlayer modes with E symmetry from the net Raman polarizability. The results are shown in Table II for the polytypes listed in Table I.

B. Compression-type modes

Iodine atoms move along the direction perpendicular to the layer for compressional (out-of-plane) modes. In contrast to the in-plane modes, the displacement pattern of these modes is the same for any pair of iodine planes A-B, A-C, and B-C and of iodine-cadmium planes. Accordingly the Raman polarizability arising from the displacements of neighboring planes will be independent of the relative configuration of neighboring iodine-iodine and iodine-cadmium planes as long as the Raman polarizability is determined mainly by the displacement of neighboring atomic planes. This means that we may regard each atomic plane as a uniform sheet for the compressional modes. In this approximation, the relative displacement and its counterphase displacement are identical. This fact leads to the result that the net Raman polarizability for the compressional modes is zero except for the $q(0)$ mode. This cancellation will occur for both intralayer and interlayer modes.

TABLE II. Calculated Raman intensities are compared with observed values. The calculated values are normalized in such a way that each intensity of intralayer and interlayer modes in the $4H$ polytype is unity. The experimental values which are divided by $[n(\omega)+1]$ are normalized to the calculated value of the most intense bands.

		Relative intensity			
		Interlayer modes		Intralayer modes	
Polytype	$\frac{c}{\pi}q$	Calculation	Observation	Calculation	Observation
$4H$	0			0	0
	1.0	1	Strong	1	Strong
$6H_1$	0			0.11	0.16 ($18R$)
$18R_1$	0.67	0.33	Strong	0.44	0.44 ($18R$)
$8H_3$	0				
	0.5	0.25	0.25	0	
	1.0	0	5.5[a]	1.0	
$12H_2$	0			0	0
$12H_4$	0.33	0.03	0.04—0.07	0.11	0.15
	0.67	0.25	0.25	0.33	0.33
	1.0	0.11	0.035—0.012	0.11	0.07
$14H_6$	0			0.51	0.51
	0.29	0.02	0.09	0.11	0
	0.57	0.068	0.11	0.11	0.16—0.22
	0.86	0.11	0.11	0.11	0.38
$42R_1$	0			0.02	0
	0.29	3.6×10^{-3}	$\sim3\times10^{-3}$	0.024	0.04
	0.57	0.02	0.023	0.052	0.05
	0.86	0.3	0.3	0.41	0.41
$16H_6$	0			0	0
	0.25	0.01	$\sim$0.009	0	0
	0.5	0	0	0	0
	0.75	0.36	0.36	0	0
	1.0	0	0.85[a]	1	Strong
$20H_{14}$	0			0.16	$\sim$0.02
	0.2	0	0	0.015	$\sim$0
	0.4	0.02	0.01	5.8×10^{-3}	$\sim$0
	0.6	0	0.08	0.1	0.06
	0.8	0.38	0.38	0.27	0.27
	1.0	0	$\sim$0	0.16	$\sim$0.05
$22H_4$	0			8.3×10^{-3}	0
	0.18	2.7×10^{-3}	$\sim10^{-3}$	2.0×10^{-3}	0.03
	0.36	2.4×10^{-3}	0.013	8.3×10^{-3}	0.03
	0.55	0.077	0.1	0.14	0.12
	0.73	0.16	0.16	0.20	0.2
	0.91	0.12	0.09	0.12	0.12

[a]Due to the $4H$-polytype component.

V. COMPARISON OF EXPERIMENTAL RESULTS WITH CALCULATION

The observed Raman intensity profiles are compared with the calculation for three polytypes $12H_2+12H_4$, $16H_6$, and $22H_4$ in Fig. 8. The computed intensities are shown by the bars which are scaled in such a way that the peak height of the most intense band coincides with the observed peak height. Correction for the Bose factor is made by multiplying the calculated values by $[n(\omega)+1]$, where $n(\omega)=[\exp(\hbar\omega/kt)+1]^{-1}$ is the Bose factor. In this figure the intensity scales for the intralayer and interlayer modes are arbitrary. The calculated result agrees with the observed Raman features qualitatively except for the 15.8-cm^{-1} band in the $16H_6$ polytype crystal, which may arise from intermixture of the $4H$ polytype. Devia-

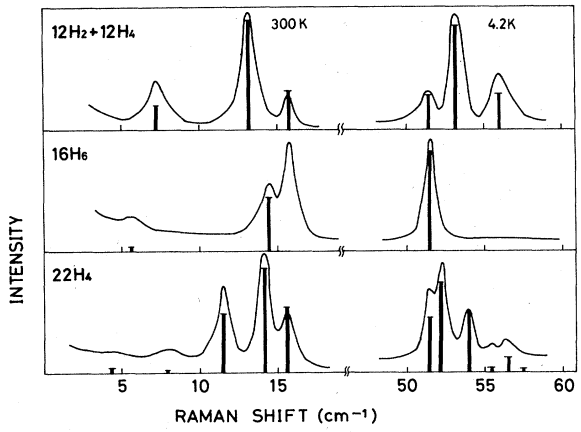

FIG. 8. Comparison of calculated intensities and observed ones for polytypes ($12H_2+12H_4$), $16H_6$, and $22H_4$. The height of bars represents the intensity which is calculated using Eq. (7). The Bose factor correction is made by multiplying the calculated intensity by $[n(\omega)+1]$.

tion from observed intensities is seen for several modes. For the interlayer modes, the deviation seems to be large for the modes with lower frequency.

Table II shows the comparison of the calculated intensity with the experimental results for ten polytypes. As seen in this table, all the modes which are predicted to be missing are not observed except the interlayer $q(\frac{2}{3})$ mode in the $20H_{14}$ polytype. The calculation indicates that the Raman intensity of the shear type modes tends to decrease in general as the period of polytypes increases.

Several modes, whose intensity is predicted not to be 0, are not observed, partly because their intensity is quite weak. However, the disappearance of the intralayer $q(\frac{2}{7})$ mode in the $14H_6$ polytype and the interlayer $q(0)$ mode in the $42R_1$ polytype does not accord with the result of the calculation. In particular, a poor agreement is observed in the $14H_6$ polytype. The reason for this disagreement is not clear at present. One of the plausible explanations is the existence of different polytypes inside the sample.

Although the deviation from the results of the calculation has been observed for some polytypes, the agreement with the theory is satisfactory considering the fact that the model employed here is oversimplified.

VI. DISCUSSION

In our model we assume that relative displacements between the nearest-neighbor planes contribute predominantly to the Raman polarizability of CdI_2 polytypes. Furthermore, for the interlayer modes, a polytype crystal is regarded as an assembly of isolated layers, but their periodicity is assumed to be retained. Despite the oversimplification, our layered-crystal model explains qualitatively the intensity profile of the Raman spectra of the folded modes and the zone-center modes in the basic zone. However, the calculated intensity profile does not coincide exactly with observation. One of the reasons is the intermixture of other polytypes. Another cause is the isolated-layer approximation. This approximation does not exactly hold in CdI_2 and the motion of the cation and the nonsymmetric movement of I-I atomic planes within a layer should be taken into account. As a matter of fact, both partners of the Davydov pair (intralayer E_1 and E_2 modes) have been observed in $4H$-PbI_2 (Refs. 4—6) and $4H$-SnS_2 (Refs. 9—11) whose layer structures are the same as that of $4H$-CdI_2. In SnS_2 the intensities of these Raman bands are comparable and the folded modes of the longitudinal acoustic branch were found.[10] These observations suggest that the isolated-layer approximation is worse in PbI_2 and SnS_2 than in CdI_2. The frequency of the shear-type interlayer mode is not separated appreciably from those of the intralayer modes in CdI_2. This fact indicates that the admixture of the interlayer and intralayer forces should be considered to some extent in CdI_2. In PbI_2 and SnS_2 these forces are admixed more strongly, though the frequency separation between the intralayer and interlayer modes is large in these crystals.

A bond polarizability model for the calculation of one- and two-phonon Raman scattering intensities for covalent crystals with the diamond structure has been proposed by Tubino and Piseri, who have used parallel and perpendicular bond polarizabilities and their first derivatives, $\alpha_{\|}$, $\alpha_{\perp}$, $\alpha'_{\|}$, and $\alpha'_{\perp}$ as parameters.[31] In the present model, we start from the standpoint that the Raman polarizabilities of the intralayer displacement for an isolated layer and of the interlayer displacement for an iodine-iodine pair are given.

It is thought that the density of states derived from phonon dispersion curves may affect the intensity of folded modes.[32] The analysis of our observation shows that the density of states does not affect the Raman intensity of the folded modes appreciably, though this effect can not be neglected.

The highest polytype of CdI_2 which could be identified so far by the Raman scattering measurement alone is the $22H$ polytype. We measured the Raman spectra of several specimens containing polytypes higher than this polytype ($n>11$). Only a few Raman bands were observed in these specimens, although a large number of folded modes are expected to appear from the zone-folding model. Some polytypes showed broad and composite Raman bands. The absence of many folded Raman bands may be due to cancellations in the Raman polarizabilities arising from relative displacements of respective nearest-neighbor atomic pairs. Our calculation has shown that the higher the polytype is, the more frequently the cancellation occurs and that the Raman intensity is reduced for many folded modes. The unresolved Raman bands in higher polytypes are considered to be formed by several folded modes which are closely spaced in frequency. The difficulty in finding fine Raman structures in higher polytypes is partly attributable to the polarizability cancellation.

In order to examine to what extent the isolated-layer approximation is valid, we have compared Raman intensities of the intralayer E_2 mode in the $4H$ polytype and the E_g mode in the $2H$ polytype. They have been determined from the intensity relative to that of the A-type intralayer mode which is considered to be equal for any CdI_2 poly-

type in the present model. The comparison has shown that the intensity of the E_2 mode is about twice as large as that of the E_g mode, whereas the model calculation indicates that both modes have the same intensity. This discrepancy arises from the restrictions in the isolated-layer approximation in which we assume that the iodine atoms in opposite planes within a layer move out of phase from each other and with the same amplitude as shown in Fig. 4, and that the Raman polarizability arising from the interlayer I-I′ displacement is negligibly small for intralayer modes. However, the amplitudes of two iodine planes are not necessarily equal in higher polytypes and cadmium atoms can also move. If the restrictions in the isolated-layer approximation are removed, we expect that the E_2 mode in the $4H$ polytype is more intense than the E_g mode in the $2H$ polytype and also that the discrepancy found in some polytypes would be removed. However, since the calculation along the line mentioned above requires more detailed lattice-dynamical calculations, it is not carried out in this paper.

VII. CONCLUSION

In this paper we have proposed a simple model based on the bond polarizability concept in order to explain the relative Raman intensities of the folded modes in CdI_2 polytypes. The Raman spectral features of the shear-type modes are interpreted qualitatively on the basis of this model. The absence of the folded modes of compression-type phonons is also explained. The relative intensity as well as the frequency of Raman bands can be used to identify the structure of CdI_2 polytypes and to determine the composition of different polytypes in a composite polytype. With a minor modification, our model can be applied equally well to other layered crystals and isotropic materials showing polytypes such as SiC. Study on several substances other than CdI_2 is now under way.

Finally, we note that although our model is essentially classical and does not provide absolute intensities, it provides a physical insight into the relative Raman intensity of layered crystals. Raman scattering intensity in addition to Raman frequency will become a source of experimental information about the nature of the atomic bonding in layered crystals, when the quantitative analysis of the Raman intensity is established.

ACKNOWLEDGMENT

The authors would like to express their sincere thanks to Professor S. Ushioda for his critical reading of the manuscript.

[1]A. R. Verma and P. Krishna, *Polymorphism and Polytypism in Crystals* (Wiley, New York, 1966).
[2]S. Montero and W. Kiefer, J. Raman Spectrosc. **1**, 565 (1973).
[3]H. Katahama, S. Nakashima, M. Hangyo, A. Mitsuishi, and B. Pałosz, Solid State Commun. **49**, 547 (1984).
[4]S. Nakashima, Solid State Commun. **16**, 1059 (1975).
[5]R. Zallen and M. L. Slade, Solid State Commun. **17**, 1561 (1975).
[6]A. Grisel and Ph. Schmid, Phys. Status Solidi B **73**, 587 (1976).
[7]W. M. Sears, M. L. Klein, and J. A. Morrison, Phys. Rev. B **19**, 2305 (1979).
[8]M. Y. Khilji, W. F. Sherman, and G. R. Wilkinson, J. Raman Spectrosc. **13**, 127 (1982).
[9]A. F. Smith, P. E. Meek, and W. Y. Liang, J. Phys. C **10**, 1321 (1977).
[10]S. Nakashima, H. Katahama, and A. Mitsuishi, Physica **105B**, 343 (1981).
[11]I. S. Gorban, V. A. Gubanov, and V. F. Orlenko, Fiz. Tverd. Tela (Leningrad) **23**, 525 (1981) [Sov. Phys.—Solid State **23**, 295 (1981)].
[12]R. M. Hoff, J. C. Irwin, and R. M. A. Lieth, Can. J. Phys. **53**, 1606 (1975).
[13]H. Yoshida, S. Nakashima, and A. Mitsuishi, Phys. Status Solidi B **59**, 655 (1973).
[14]A. Polian, K. Kunc, and A. Kuhn, Solid State Commun. **19**, 1079 (1976).
[15]For other papers related to this subject, see T. J. Wieting and J. L. Verble, in *Electrons and Phonons in Layered Crystal Structures,* edited by T. J. Wieting and M. Schluter (Reidel, Dordrecht, 1979), p. 321.
[16]D. W. Feldman, J. H. Parker, Jr., W. J. Choyke, and L. Patrick, Phys. Rev. **170**, 698 (1968).
[17]D. W. Feldman, J. H. Parker, Jr., W. J. Choyke, and L. Patrick, Phys. Rev. **173**, 787 (1968).
[18]H. Katahama, S. Nakashima, A. Mitsuishi, and B. Pałosz (unpublished).
[19]For SiC the unfolded zone has been previously called the "large zone." See Ref. 16.
[20]S. Nakashima, H. Katahama, M. Daimon, and A. Mitsuishi, Solid State Commun. **36**, 913 (1979).
[21]P. E. Schmid, in *Festkörperprobleme* (Advances in Solid State Physics), edited by J. T. Dortmund (Pergamon, Braunschweig, 1976), p. 74, Vol. XVI.
[22]In Ref. 14, Wieting and Verble stated that the E_g mode in the $2H$ polytype corresponds to the E_2 mode in the $4H$ polytype. Their statement in Fig. 5.7 of this reference, which results from a misassignment, is incorrect. The displacement patterns of the E_1^3 and E_2^3 modes should be interchanged.
[23]B. Pałosz, J. Cryst. Growth **52**, 969 (1981).
[24]R. S. Mitchel, Z. Kristallogr. **108**, 296 (1956).
[25]T. Minagawa, Acta Crystallogr. A **34**, 243 (1978).
[26]P. C. Jain and G. C. Trigumayat, J. Cryst. Growth **48**, 10 (1980).
[27]B. Pałosz, Acta Crystallogr. B **38**, 3001 (1982).
[28]B. Pałosz, Z. Kristallogr. **153**, 51 (1980).
[29]H. J. L. van der Waals and C. Haas, Phys. Status Solidi B **80**, 321 (1977).
[30]A. Frey and R. Zeyher, Solid State Commun. **28**, 435 (1978).
[31]R. Tubino and L. Piseri, Phys. Rev. B **12**, 5145 (1975).
[32]E. A. Vinogradov, G. N. Zhizhin, N. N. Melnik, S. I. Subbotin, V. V. Panfilov, K. R. Allakhverdiev, S. S. Babaev, and V. F. Zhitar, Phys. Status Solidi B **99**, 215 (1980).